AD-A099 278 COLORADO STATE UNIV FORT COLLINS DEPT OF CHEMISTRY F/G 20/10
ON THE LOWEST EXCITED SINGLET STAT EOF OSMIUM TETROXIDE.(U)
MAR 81 K M SWIFT, E R BERNSTEIN N00014-79-C-0647
UNCLASSIFIED TR-3 NL

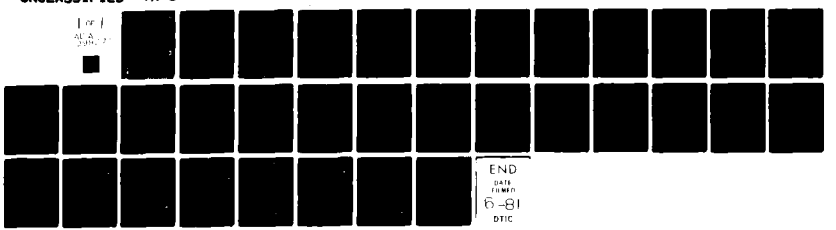

END
DATE FILMED
6-81
DTIC

II

12

OF NAVAL RESEARCH

Contract N00014-79-C-0647

Technical Report No. 3

TR-3

ON THE LOWEST EXCITED SINGLET STATE OF OSMIUM TETROXIDE

by

K. M. SWIFT and E. R. BERNSTEIN

Prepared for Publication in
The Journal of Chemical Physics

Department of Chemistry
Colorado State University
Fort Collins, Colorado 80523

10 February 1981

UNCLASSIFIED

SECURITY CLASSIFICATION OF THIS PAGE (When Data Entered)

REPORT DOCUMENTATION PAGE		READ INSTRUCTIONS BEFORE COMPLETING FORM
1. REPORT NUMBER: Technical Report No. 3 ✓	2. GOVT ACCESSION NO.: AD-A099278	3. RECIPIENT'S CATALOG NUMBER
4. TITLE (and Subtitle): ON THE LOWEST EXCITED SINGLET STATE OF OSMIUM TETROXIDE		5. TYPE OF REPORT & PERIOD COVERED: TECHNICAL REPORT
		6. PERFORMING ORG. REPORT NUMBER
7. AUTHOR(s): K.M. SWIFT and E.R. BERNSTEIN		8. CONTRACT OR GRANT NUMBER(s): N00014-79-C-0647 ✓
9. PERFORMING ORGANIZATION NAME AND ADDRESS: Department of Chemistry ✓ Colorado State University Fort Collins, Colorado 80523		10. PROGRAM ELEMENT, PROJECT, TASK AREA & WORK UNIT NUMBERS
11. CONTROLLING OFFICE NAME AND ADDRESS: Office of Naval Research Arlington, Virginia 22217		12. REPORT DATE: March 10, 1981
		13. NUMBER OF PAGES: 34
14. MONITORING AGENCY NAME & ADDRESS (if different from Controlling Office)		15. SECURITY CLASS. (of this report): UNCLASSIFIED
		15a. DECLASSIFICATION/DOWNGRADING SCHEDULE

16. DISTRIBUTION STATEMENT (of this Report)

Approved for Public Release; Distribution Unlimited.

17. DISTRIBUTION STATEMENT (of the abstract entered in Block 20, if different from Report)

18. SUPPLEMENTARY NOTES

19. KEY WORDS (Continue on reverse side if necessary and identify by block number)

nu sub 3, nu' sub 3 - 588/cm (nu'' sub 3 = 1/960 cm)

27295/cm

20. ABSTRACT (Continue on reverse side if necessary and identify by block number)

Two photon spectra of OsO_4 in the region below the first strong one photon transition are oberved and analyzed. The data fit a linear Jahn-Teller (Txt) calculation. An assignment of the two photon features as arising from a T_{2u} (sub 2) electronic state, origin at 27,295 cm^{-1}, with a dominant linear Jahn-Teller active t2 vibration (ν_3, ν_3, =588cm^{-1}, (ν_3'' = 960 cm^{-1}), and with Jahn-Teller parameter D=0.5 is proposed. Based on these findings the two observed one photon states are discussed and qualitatively analyzed in a parallel fashion.

DD FORM 1 JAN 73 1473 EDITION OF 1 NOV 65 IS OBSOLETE

UNCLASSIFIED

SECURITY CLASSIFICATION OF THIS PAGE (When Data Entered)

ON THE LOWEST EXCITED STATE OF OSMIUM TETROXIDE

by

K.M. SWIFT and E.R. BERNSTEIN

Department of Chemistry
Colorado State University
Fort Collins, Colorado 80523

ABSTRACT

Two photon spectra of OsO_4 in the region below the first strong one photon transition are observed and analyzed. The data fit a linear Jahn-Teller (Txt) calculation. An assignment of the two photon features as arising from a T_1 electronic state, origin at 27,295 cm^{-1}, with a dominant linear Jahn-Teller active t_2 vibration ν_3, ν_3'=588 cm^{-1} (ν_3'' = 960 cm^{-1}), and with Jahn-Teller parameter D=0.5 is proposed. Based on these findings the two observed one photon states are discussed and qualitatively analyzed in a parallel fashion.

I. INTRODUCTION

Osmium and ruthenium tetroxides (OsO_4, RuO_4) have been the subjects of intense investigation for many years. Ultraviolet absorption [1-14], photoelectron spectroscopy [15-17], and magnetic circular dichroism (MCD) [11-13,18] have all been used to probe the electronic structure of these molecules.

OsO_4 and RuO_4 are of interest as members of a large class of tetrahedral, isoelectronic "tetroxo" compounds (MO_4^{n-}; M=Cr,Mo,W,Mn,Tc,Re,Ru,Os). These compounds all show intense dipole allowed transitions in the visible or ultraviolet. For the point group T_d, the dipole operator transforms as T_2, so these allowed states are assigned as being of T_2 symmetry.

There is general consensus that the molecular orbital scheme shown in Figure 1 holds for these compounds. As shown in the figure, the lowest energy electron promotion $e \leftarrow t_1$ yields both T_1 and T_2 electronic states. The first strong one-photon transition can then be assigned as being of the $e \leftarrow t_1$ type. The t_1 orbital has mainly nonbonding oxygen atomic orbital character. The e orbital is composed mainly of osmium 5d orbitals, which have been split by the ligand field into a lower e orbital and upper t_2 orbital. Transitions involving these orbitals are commonly called charge transfer transitions, since an electron is transferred from the oxygen atom to the osmium atom.

The other state arising from the electron promotion $e \leftarrow t_1$, namely the T_1 state, has been observed for the permanganate ion (MnO_4^-) through careful crystal studies [19-20] and MCD spectroscopy[21]. It is weak and lies well below the first intense transition.

We have investigated the low-lying regions of the OsO_4 spectrum from 25,000-32,300 cm^{-1} using the technique of two photon gas phase fluorescence excitation spectroscopy in an attempt to find new information about the electronic structure of OsO_4.

II. EXPERIMENTAL

The tunable laser for these experiments was a Nd/YAG pumped dye laser (Quanta-Ray DCR-1A and PDL). Five dyes were necessary to cover the entire range of reported spectra. In order to obtain sufficient power in the low energy region from 25,000 to 28,000 cm^{-1}, it was necessary to Raman shift (in high pressure H_2) the output of Rhodamine 640,610, and 590 (Exciton). For the region from 27,700-30,100 cm^{-1} a special experimental dye related to DCM was kindly donated to us by Exciton Chemical Company, Inc.; DMSO was the solvent used. For 29,900 to 32,300 cm^{-1} Exciton DCM was used.

Spectra were obtained by monitoring emission from the sample following excitation. Input power was between 2 and 10 mJ/pulse. Emission was detected perpindicular to the focused incident beam by an RCA 8850 photomultiplier tube protected by two Hoya B-390 filters and a 1.0 cm pathlength of 80% saturated $CuSO_4 \cdot 5H_2O$ in water (250 g/l). The output of the phototube was put directly into the A channel of a boxcar integrator (PAR 164/162). Dye laser power was monitored by a silicon photodiode, whose output was put directly into the B channel of the boxcar integrator. The spectra were obtained by scanning the dye laser under computer control, and sampling the output of the two channels of the boxcar integrator for several laser pulses at each wavelength. Normalization for the square power dependence characteristic of two photon absorption was accomplished by dividing the signal channel (A) by the square of the power channel (B). In addition, the optogalvanic spectrum of an Fe-Ne hollow cathode lamp was recorded simultaneously for calibration purposes. Between five and thirty scans over the dye's range were averaged, depending on the signal to noise ratio. Circularly polarized light was obtained with a Fresnel rhomb.

The material used was commercial OsO_4, purified further by distillation

under high vacuum through 4 Å molecular sieve. OsO_4 reacts with grease, so a grease free vacuum manifold was used. The sample cell was filled with the full vapor pressure at room temperature (21°C). Vapor pressure was measured to be about 5 torr with a Baratron gauge.

III. RESULTS AND DISCUSSION

The observed spectrum is shown in survey form in Figs. 2,3 and the complete data are tabulated in Table 1. There are no features until about 26,800 cm^{-1}, at which point a very complicated spectrum begins. The spectrum extends into the region of the first strong one photon state which begins at 31,359 cm^{-1}.[8]

In an attempt to elucidate the vibrational parentage of the transitions, emission from the sample excited at two pump energies, 31,830 cm^{-1} and 30,582 cm^{-1}, was dispersed in a 1 meter monochrometer. Emission was found not to be from the molecule, OsO_4, but from neutral osmium atoms (Os(I)). No molecular emission could be found. Still, the excitation spectra that were obtained could be genuine two photon OsO_4 spectra, if in fact the rate-limiting step for the dissociation followed by emission is the initial two photon absorption by OsO_4.

This situation is not without precedent. For example, pyrazine and triazine two photon spectra have been obtained by monitoring the emission from cyanyl (CN) produced by photodecomposition of the sample by the laser.[22,23] However, the possibility of contamination of the spectrum by the photoproducts exists. Thus, the spectrum must be analyzed as OsO_4 in order to prove that it is entirely due to OsO_4.

In order to assign the spectrum, we must consider the two photon selection rules. McClain and Harris have given an excellent treatment of this problem.[24] Properties of the two photon transition tensor give both selection rules and polarization behavior. In short, the transition is allowed for identical photons if the transition tensor is symmetric; it is circularly polarized if the tensor has a non-zero trace. These results are applied to the group T_d in Table 2. Also contained in Table 2 are the ΔK selection rules obtained by the method given by McClain and Harris.

Rotational contours can be quite useful for symmetric top assignments,

since a one to one correspondence exists between ΔK selection rules and vibronic symmetry.[25,26] For the spherical top, on the other hand, the K levels are degenerate; thus for a given energy, symmetric top intensity factors must be summed subject to ΔK selection rules. In the notation of reference 26:

$$|J'> \leftarrow |J>: \quad W = \sum_{KK'} W_{J'K',JK} = \sum_{KK'} (C_0 M_0 R_0 + C_2 M_2 R_2)$$

in which $R_0 = \delta_{JJ'}\delta_{KK'}$ and $R_2 = b^{JK}_{J'K'}$ the Placzek-Teller coefficient.[27]

Summation of symmetric top factors is accomplished using the following relations:

$$\Sigma_{KK'} \delta_{JJ'} \delta_{KK'} = (2J+1)$$
$$\Sigma_K b^{JK}_{J'K'} = (2J' + 1)/5 \text{ (for a given } \Delta K).$$

The latter relation is first derived in reference 27. The result is that the formulas for the intensity work out similarly for $E \leftarrow A_1$ and $T_2 \leftarrow A_1$:

$$E \leftarrow A_1 \qquad W = \frac{C_2}{5}(2J' + 1)\left[|M^2_{+2}|^2 + |M^2_{-2}|^2 + |M^2_0|^2\right],$$

$$T_2 \leftarrow A_1 \qquad W = \frac{C_2}{5}(2J' + 1)\left[|M^2_{+2}|^2 + |M^2_{-2}|^2 + |M^2_{+1}|^2 + |M^2_{-1}|^2\right],$$

$$A_1 \leftarrow A_1 \qquad W = C_0 (2J+1) |M^0_0|^2.$$

Rotational contours can thus distinguish between $A_1 \leftarrow A_1$ and $E \leftarrow A_1$ or $T_2 \leftarrow A_1$, but not between $E \leftarrow A_1$ and $T_2 \leftarrow A_1$.

Expressions for the energy and coriolis coupling of a spherical top may be found in references 28 and 29. Employing these formulas, calculation of rotational contours proceeds in the standard fashion.[25,26] Some experimental and theoretical rotational contours are presented in Fig. 4,5 and 6. Note that the contours extend over about 50 cm^{-1}. This would seem to eliminate the

possibility of atomic two photon absorption spectra arising from photogenerated atomic species (Os(I)), such as was reported in references 30 and 31.

It is clear that calculated contours of 3_0^1 (T_2) (Fig. 4) and the 29373, 29440 and 29517 cm^{-1} features (Fig. 5) agree only fairly well with the experimental ones. The experimental bands are somewhat simpler than the calculated ones. This situation occurs for some of the other features, as well. It should be noted that a diatomic or triatomic symmetric top model, which might be appropriate for photo product absorption, generates a poorer rotational contour fit in all instances. Since this region of the spectrum of OsO_4 produces a good deal of photochemical activity, it is quite reasonable to assume that certain contour features are lost due to lifetime broadening.

To fit the feature at 28,800 cm^{-1} it was necessary to overlap two totally symmetric contours of different moments of inertia with origins separated by 60 cm^{-1} (Fig 6). In fact the lower energy feature has a moment of inertia 7% larger than the ground state and the high energy feature has a moment of inertia 7% lower than the ground state. Such changes are typical of Jahn-Teller perturbed systems and have been noted before.[23] The agreement between the overlapped calculated contours and the experimental feature is quite reasonable. (See discussion below).

The strongest argument for the spectrum being due to OsO_4 is that the first nine major features fit the Jahn-Teller ($T_1 x t_2$) vibronic calculation of Caner and Englman[32] nearly exactly (average deviation = 11 cm^{-1}) for a parameter value $k=L/\sqrt{6}\hbar\omega = 1.0$ or $D = 0.5$ (see Fig. 7). For a comparison of calculated and experimental features, refer to Table 3. The value of the unperturbed excited state frequency is 588 cm^{-1}, so the vibration must be ν_3', whose ground state frequency is 960 cm^{-1} (see Table 4). The other t_2 vibration, ν_4', is too low in energy (329 cm^{-1} in the ground state) to be considered for this series.

Two other pieces of information fit in well with the above interpretation. First, the seventh peak in the progression (28792 cm^{-1}) is polarized, in accordance

with the calculated feature of A_1 symmetry predicted to lie at 28809 cm^{-1}. As was mentioned earlier, the contour is a combination of two polarized features. We assume that the lower one is $3_0^3(A_1)$. Second, the forbidden T_1 origin is predicted to lie at 27295 cm^{-1}, and a ~330 cm^{-1} hot band appears to be built on this position as it should be, since $2_1^0(T_1 \leftarrow E)$ and $4_1^0(T_1 \leftarrow T_2)$ will be allowed. Hot bands located 330 cm^{-1} below the major features are not generally found, however, presumably because they involve a change in quanta for two vibrations, ν_3 and ν_2 or ν_4. The Boltzmann factor for ν_3 hot bands is very unfavorable.

Intensities for the $[T_1 \times t_2]$ ν_3 manifold are qualitatively in agreement with the n=1 coefficients of the computed eigenvectors, as would be expected for a Herzberg-Teller vibronic coupling intensity mechanism.[23] For example, the following predictions (See Table III) can be accurately made: $3_0^3(A_1)$ at ~28,800 cm^{-1} is quite intense; $3_0^2(T_2)$ at 28316 cm^{-1} is less intense than $3_0^2(E)$ at 28483 cm^{-1}; and $3_0^3(T_2)$ at 28981 cm^{-1} is less intense than $3_0^3(E)$ at 29069 cm^{-1}. Other trends in these data are also predicted correctly by the eigenvector calculations.

Thus, nine energies and intensities, plus two additional pieces of information are fit by two parameters, the linear Jahn-Teller coupling strength and the excited frequency. The fact that one vibration should dominate the entire spectrum is similar to the situation in triazine, for which ν_6 dominates the spectrum.[23] What is unusual here, however, is the absence of any totally symmetric progression built on the ν_3 series.

The one photon spectrum also lacks a well defined totally symmetric progression[8], through at first glance the spectrum appears to possess a long series in ν_1. It may be that ν_3 perturbs the one photon spectrum as well. In fact, the first six $T_2 \times t_2$ vibronic coupling calculation T_2 levels actually fit the first few one photon features fairly well (average deviation 43 cm^{-1}) for a parameter value $k=L/\sqrt{6}\,M\omega = 1.0$ or D=0.5 and $\omega_3' = 736$ cm^{-1} (see Table V). This good agreement indicates that ν_3 is involved in the progression in the lower T_2 state. These conclusions are consistent with those reached through MCD studies of both MnO_4^- [33]

and OsO_4.[11,12] The value of the Jahn-Teller parameter for the lower T_2 state is about a factor of two larger than that of MnO_4^- (D=0.27).[33]

Our two photon data also support this conclusion, as there is an intense polarized feature at 31827 cm^{-1} and the calculation gives a one photon forbidden A_1 vibronic symmetry feature at 31846 cm^{-1}. This is the only predicted A_1 $[T_2 \times t_2]$ level within $\pm$ 1000 cm^{-1} of the observed feature.

One can then examine the second intense transition beginning at 38733 cm^{-1} for possible agreement with the calculation. For D=1.1 and $\nu_3' = 754$ cm^{-1}, one again finds agreement (see Table VI) with an average deviation of 31 cm^{-1}. We therefore believe that the irregularities in the progression intervals in the one photon data are due to a linear Jahn-Teller perturbed ν_3' (t_2) manifold in both T_2 electronic states. However, due to the diffuse nature of the one photon spectrum, conclusive proof for this apparently reasonable conclusion must await further spectroscopic studies now in progress.

The ν_3 vibration involves the central osmium atom moving in one direction, with the oxygen atoms moving in the opposite direction. The mode is the only one involving movement of the osmium atom. Therefore, it is to be expected that ν_3 would be quite important for vibronic coupling (both Herzberg-Teller and Jahn-Teller) in a charge transfer transition.

We are continuing the investigation of two photon features in the one photon region. We also plan to employ the photoacoustic detection method in order to gain further information with regard to the photophysics and photochemistry of this system.

IV. CONCLUSIONS

A low lying T_1 state of OsO_4 has been observed by two photon spectroscopy. The spectrum is dominated by a Jahn-Teller perturbed $\nu_3(t_2)$ vibrational progression. This interpretation is strongly supported by the T_1 xt_2 vibronic coupling calculation of Caner and Englman, which gives the location of the T_1 electronic origin as 27295 cm^{-1}, $\nu_3' = 588$ cm^{-1}, and D = 0.5. Both one photon allowed T_2 states are also qualitatively interpretable in terms of these concepts. Finally, OsO_4 is observed to be photochemically active, producing neutral osmium atoms which then emit.

V. ACKNOWLEDGMENT

We wish to thank Dr. R. Englman for providing us with a copy of his k=1 eigenvalue and eigenvector calculation for [T x t].

REFERENCES

1. J. Lifschitz and E. Rosenbohm, Z. phys. Chem. 97, 1 (1921).
2. S. Kato, Scientific Papers of the Institute of Physical and Chemical Research 13, 249 (1930).
3. A. Langseth and B. Qviller, Z. phys. Chem. B 27, 79 (1934).
4. S.E. Krasikov, A.N. Filippov, and I.I. Chernyaev, Izv. Sekt. Platiny drug. blagor. Metall. Inst. obshchei neorg. Khim. 13, 19 (1936).
5. B. Qviller, Tidsskr. Kjemi Bergv. Metall. 17, 127 (1937).
6. R.E. Connick and C.R. Hurley, J. Am. Chem. Soc. 74, 5012 (1952).
7. G.B. Barton, Spectrochem. Acta. 19, 1619 (1963).
8. E.J. Wells, A.D. Jordan, D.S. Alderdice, and I.G. Ross, Aust. J. Chem. 20, 2315 (1967).
9. A. Mueller and E. Diemann, Chem. Phys. Lett. 9, 369 (1971).
10. S. Foster, S. Felps, L.W. Johnson, D.B. Larson, and S.P. McGlynn, J. Am. Chem. Soc. 95, 6578 (1973).
11. T.J. Barton, R. Grinter, and A.J. Thomson, Chem. Phys. Lett. 40, 399 (1976).
12. P. Quested, D.J. Robbins, P. Day, and R.G. Denning, Chem. Phys. Lett. 22, 158 (1973).
13. R.H. Petit, B. Briat, A. Mueller, and E. Diemann, Mol Phys. 27, 1373 (1974).
14. W.H. Beattie, W.B. Maier, R.F. Holland, S.M. Freund, and B. Stewart, SPIE Proceedings 158 (Laser Spectroscopy), 113 (1978).
15. E. Diemann and A. Mueller, Chem. Phys. Lett. 19, 538 (1973).
16. S. Foster, S. Felps, L.C. Cusachs, and S.P. McGlynn, J. Am. Chem. Soc. 95, 5521 (1973).
17. P. Burroughs, S. Evans, A. Hamnett, A.F. Orchard, and N.V. Richardson, J. Chem. Soc., Faraday Trans. II 70, 1895 (1974).
18. R.H. Petit, B. Briat, A. Mueller, and E. Diemann, Chem. Phys. Lett. 20, 540 (1973).

19. P. Day, L. Disipio, and L. Oleari, Chem. Phys. Lett. 5, 533 (1970).

20. L.W. Johnson, E. Hughes, Jr., and S.P. McGlynn, J. Chem. Phys. 55, 4476 (1971).

21. J.C. Collingwood, P. Day, R.G. Denning, D.J. Robbins, L. Disipio, and L. Oleari, Chem. Phys. Lett. 13, 567 (1972).

22. J.D. Webb, K.M. Swift, and E.R. Bernstein, J. Mol. Struct. 61, 285 (1980).

23. J.D. Webb, K.M. Swift, and E.R. Bernstein, J. Chem. Phys. 73, 0000 (1980).

24. W.M. McClain, and R.A. Harris, Excited States, edited by E.C. Lim (Academic, New York, 1977), Vol 3, p. 1-56.

25. L. Wunsch, F. Metz, H.J. Neusser, and E.W. Schlag, J. Chem. Phys. 66,386 (1977).

26. F. Metz, W.E. Howard, L. Wunsch, H.J. Neusser, and E.W. Schlag, Proc. R. Soc. (London) A363, 381 (1978).

27. G. Placzek and E. Teller, Z. Phys. 81, 209 (1933).

28. H.C. Allen Jr. and P.C. Cross, Molecular VIB-ROTORS (Wiley-Interscience, New York, 1963).

29. F.N. Masri and W.H. Fletcher, J. Chem. Phys. 52, 5759 (1970).

30. D.P. Gerridy, L.J. Rothberg, and V. Vaida, Chem. Phys. Lett. 74, 1 (1980).

31. S. Leutwyler, U. Even, and J. Jortner, Chem. Phys. Lett. 74, 11 (1980).

32. R. Englman, The Jahn-Teller Effect in Molecules and Crystals (Wiley-Interscience, New York, 1972) p. 72.

33. P.A. Cox, D.J. Robbins, and P. Day, Mol. Phys. 30, 405 (1975).

TABLE I. Tabulation and assignment of observed two photon energy levels of OsO_4 T_1 first excited electronic state.

$2\sigma_{vac}$ (cm-1)	Intensity [a]	Assignment
26805	VW	
26965	W	$2_1^0(T_1 \leftarrow E)$, $4_1^0(T_1 \leftarrow T_2)$
27041	VW	
27141	VW	
27568	VW	$2_0^1(T_2)$ or $4_0^1(T_2)$
27745	M	$3_0^1(T_2)$
27790	VW	
27955	VW	
27984	M	$3_0^1(E)$
28108	VW	
28217	VW	
28316	W	$3_0^2(T_2)$
28483	M	$3_0^2(E)$
28562	W	$3_0^2(T_2)$
28627	W	$3_0^3(E)$
28792[b]	S	$3_0^3(A_1)$
28843[b]	S	
28981	M	$3_0^3(T_2)$
29054[b]	S	
29069	S	$3_0^3(E)$
29160	M	
29182	M	
29235	M	

(Continued....)

TABLE I (continued)

$2\sigma_{vac}$ (cm-1)	Intensity [a]	Assignment
29373	S	
29440	VS	
29517	S	
29771	M	
29848	M	
30025	S	
30119	M	
30161	M	
30226	M	
30298	M	
30363	M	
30403	M	
30447	M	
30582	VS	
30729	M	
30850	M	
31028	M	
31054	M	
31197	M	
31254	VS	
30358	S	
31381	S	
31486	M	
31827 [b]	VVS	$3_0^1(A_1)$ [T_2]
31974	M	

(Continued....)

TABLE I. (continued)

$2\sigma_{vac}$ (cm-1)	Intensity [a]	Assignment
32034	VS	
32171	M	
32241	M	

FOOTNOTES

(a) w=weak, vw=very weak, m=medium, s=strong, vs=very strong, vvs=very very strong

(b) changes intensity with circularly polarized light

TABLE II. Polarization and Selection rules for two photon transitions in T_d symmetry.

Vibronic Symmetry	ΔK Selection Rule	Polarization Behavior
$A_1 \leftarrow A_1$	$\Delta K=0$	Completely Polarized
$E \leftarrow A_1$	$\Delta K=0,\pm 2$	Unpolarized
$T_2 \leftarrow A_1$	$\Delta K=\pm 1,\pm 2$	Unpolarized

TABLE III. Comparison of observed and calculated[32] $\nu_3(t_2)$ vibronic components in the lowest excited T_1 electronic state of OsO_4 (in cm^{-1}). Parameter values are: ν_3= 588 cm^{-1} and k=1.0 (D=0.5).

Assignment	Observed	Calculated[a]	n=1 Eigenvector Coefficient [a]
4_1^0 $(T_1 \leftarrow T_2)$ 2_1^0 $(T_1 \leftarrow E)$	26965	[26965][b]	-
(0,0)	[27295][c]	27295	-
$3_0^1(T_2)$	27745	27746	0.70857
$3_0^1(E)$	27984	27978	0.64057
$3_0^2(T_2)$	28316	28314	0.18714
$3_0^2(E)$	28483	28488	0.58802
$3_0^2(T_2)$	28562	28559	0.42760
$3_0^3(E)$	28627	28642	0.36891
$3_0^3(A_1)$[d]	28792	28809	0.63308
$3_0^3(T_2)$	28981	28942	-0.092403
$3_0^3(E)$	29069	29081	-0.27411

a) values supplied by R. Englman; see ref. 32

b) calculated by subtracting 330 cm^{-1} from origin

c) forbidden. calculated from hot bands 2_1^0,4_1^0

d) observed and predicted to be polarized

TABLE IV. Ground state OsO_4 vibrations

ν_1	a_1	symmetric stretch	965 cm^{-1}
ν_2	e	bend	333
ν_3	t_2	asymmetric stretch	960
ν_4	t_2	bend	329

TABLE V. Comparison of one photon data[8] for T_2 state of OsO_4 with vibronic coupling $T_2 \times t_2$ calculation[32] (D=0.5, $\nu_3' = 736\ cm^{-1}$). sh, shoulder; p, peak. Frequencies in cm-1. Error in frequencies 5-20 cm-1.

Band [a]	Observed	Calculated[c]
A	31261 sh	
	31359 p	31294 (T_2)
	31398 sh	
A-B	31661 sh	
	[31827 p (A_1)] [b]	31846 (A_1)
B	32093 sh	
	32197 p	32305 (T_2)
B-C	32479 p	32489 (T_2)
C	32950 sh	32931 (T_2)
	33059 p	33041 (T_2)
C-D	33297 p	33262 (T_2)

a. Ref. 8 band designations

b. Observed two photon peak, this work

c Measured from ref. 32 figure ($\pm$ 20 cm^{-1})

TABLE VI. Comparison of one photon data[8] for the upper T_2 state of OsO_4 with vibronic coupling $T_2 \times t_2$ calculation.[32] (D=1.1 $\nu_3' = 754\ cm^{-1}$). sh, shoulder; p, peak. Frequencies in cm^{-1}. Error in frequencies 5-20 cm^{-1}.

Band [a]	Observed	Calculated [b]
K	38421 sh	
	38509 sh	
	38643 sh	
	38733 p	38743
	38906 sh	
K-L	39112 sh	
L	39381 sh	
	39523 sh	
	39592 p	39573
	39765 p	39742
L-M	40100 sh	40139
M	40433 p	40478
	40605 p	40553

a. Ref. 8 band designations

b. Measured from ref. 32 figure ($\pm$ 20 cm^{-1}).

FIGURE CAPTIONS

Figure 1 - Molecular orbital scheme for OsO_4. The bottom part of the figure shows the electronic states arising from certain electronic transitions. The lower filled orbitals are drawn to scale and are determined by photo-electron spectroscopy.[17]

Figure 2 - Survey two photon photochemi-luminescence spectrum of OsO_4. Bracketed area is expanded in Figure 3.

Figure 3 - First 2000 cm^{-1} of two photon photochemi-luminescence spectrum of OsO_4. Assignments for this region, given by a linear Jahn-Teller calculation, label various features.

Figure 4 - Rotational contour for $3_0^1(T_2)$.

a. Experimental, single scan of feature. Weak peak to high energy side of 3_0^1 is not part of the 3_0^1 contour.

b. Calculated contour with $B''=0.1349\ cm^{-1}$ $B'=0.13\ cm^{-1}$ $\zeta=-0.6$

Figure 5 - Rotational contours for 29373, 29440, 29517 cm^{-1} features:

a. Experimental features, single scan

b. Calculated for feature at left - $B''=0.1349\ cm^{-1}$, $B'=0.13\ cm^{-1}$, $\zeta=-1.0$

c. Calculated for central feature - $B''=0.1349\ cm^{-1}$, $B'=0.128\ cm^{-1}$, $\zeta=-0.6$

d. Calculated for $B''=0.1349\ cm^{-1}$, $B'=0.128\ cm^{-1}$, $\zeta=-0.4$

Figure 6 - Rotational contour for $3_0^1(A_1)$:

a. Experimental (Seven Scans).

b. Calculated with two overlapping A_1 bands probably $3_0^3(A_1)$ and $3_0^4(A_1)$-$B''=0.1349\ cm^{-1}$ $B_1'=0.145\ cm^{-1}$, $B_2'=0.125\ cm^{-1}$, with origins separated by 60 cm^{-1}. Higher energy contour weighted with an intensity factor 0.7 that of the lower energy contour.

Figure 7 - Vibronic energy levels for $T_2 \times t_2$ from ref. 32. For a T_1 electronic state all 1 and 2 subscripts are interchanged. Vertical axis in units of $\hbar\omega$.

MOLECULAR ORBITALS

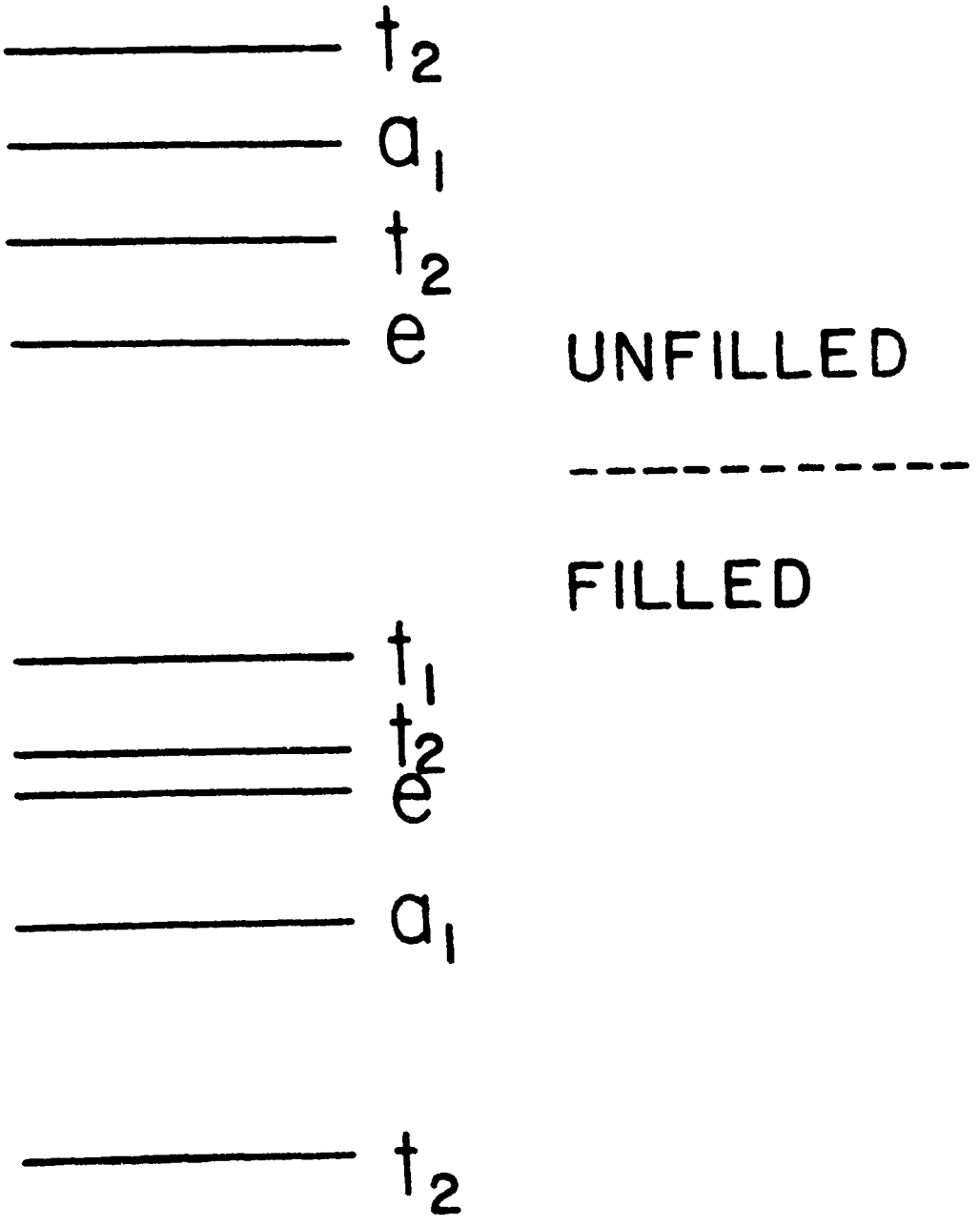

$t_1 \rightarrow e$: T_1, T_2

$t_1 \rightarrow t_2$: A_2, E, T_1, T_2

Fig 1

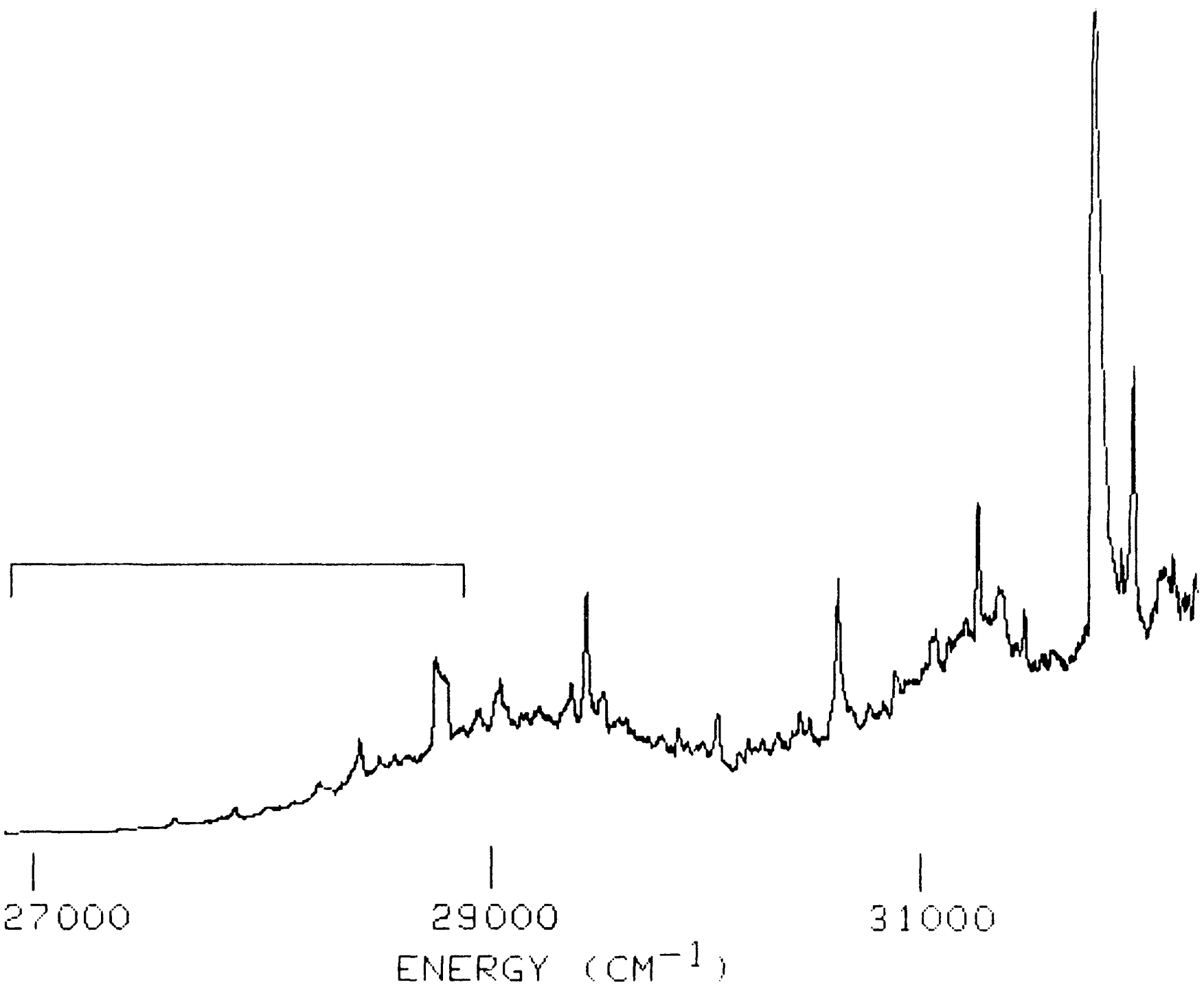

Fig 2

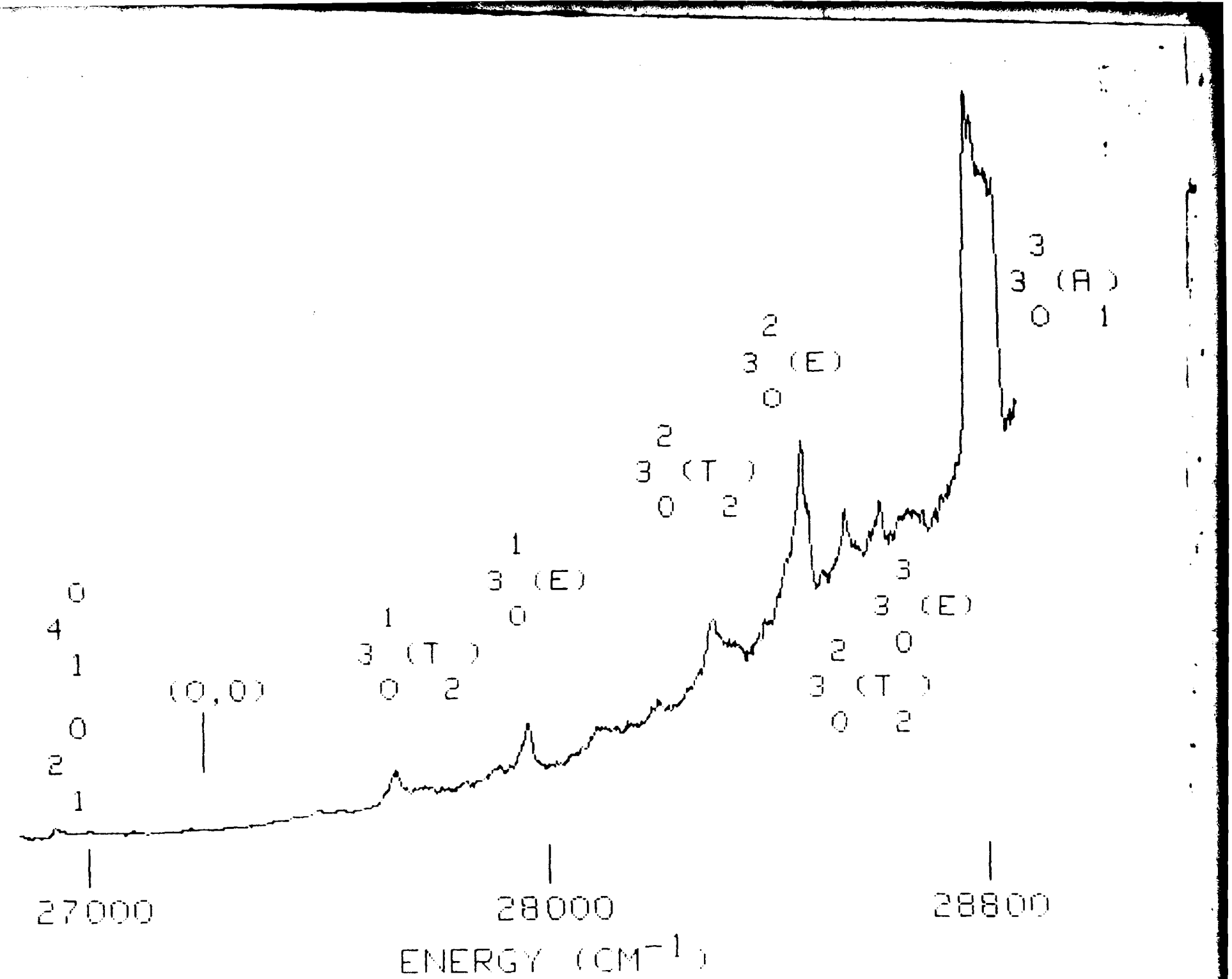
0
4
1
0
2
1
(0,0)
1
3 (T)
0 2
1
3 (E)
0
2
3 (T)
0 2
2
3 (E)
0
3
3 (E)
2 0
3 (T)
0 2
3
3 (A)
0 1
27000
28000
28800
ENERGY (CM-1)

Fig 3

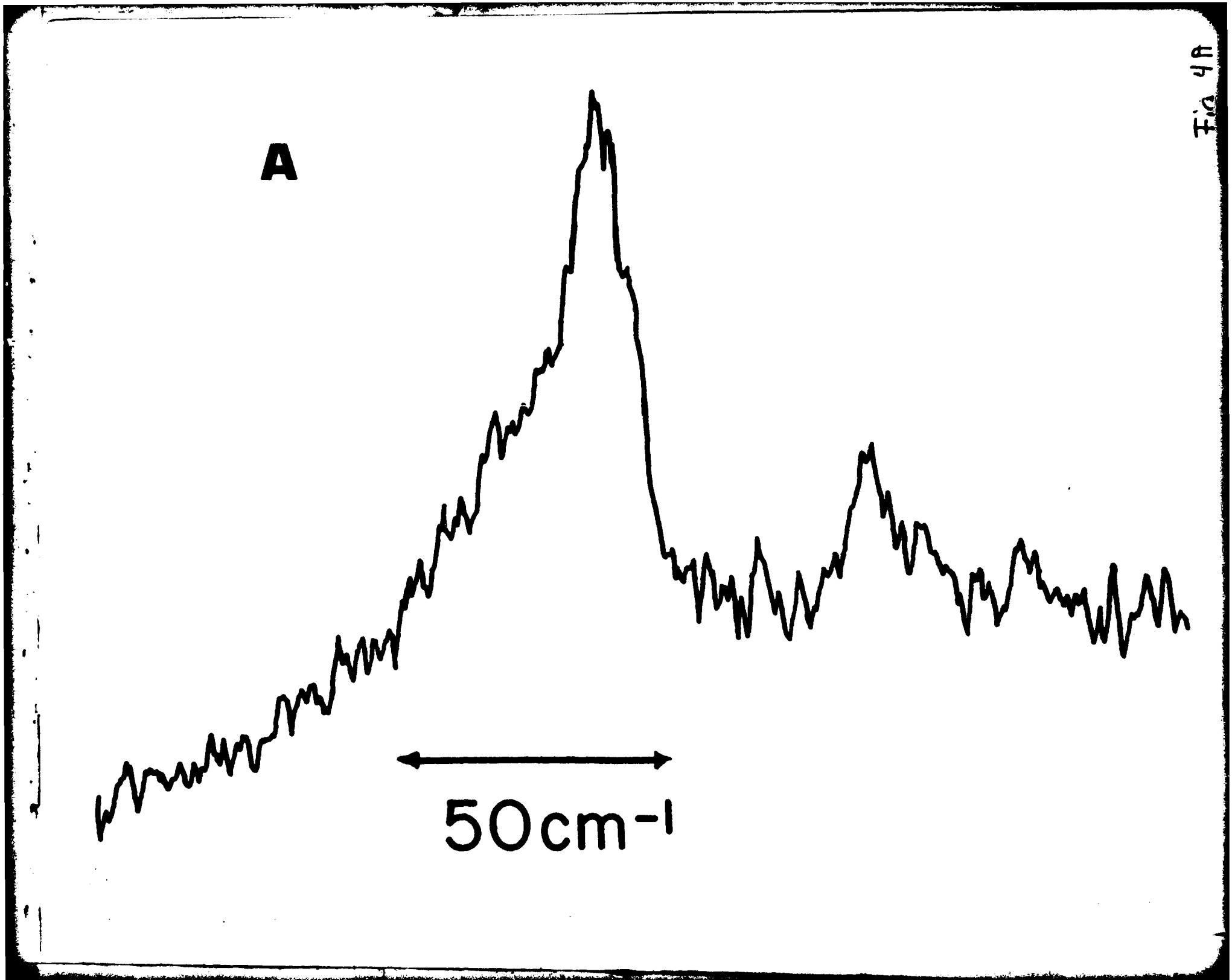

Fig 4A

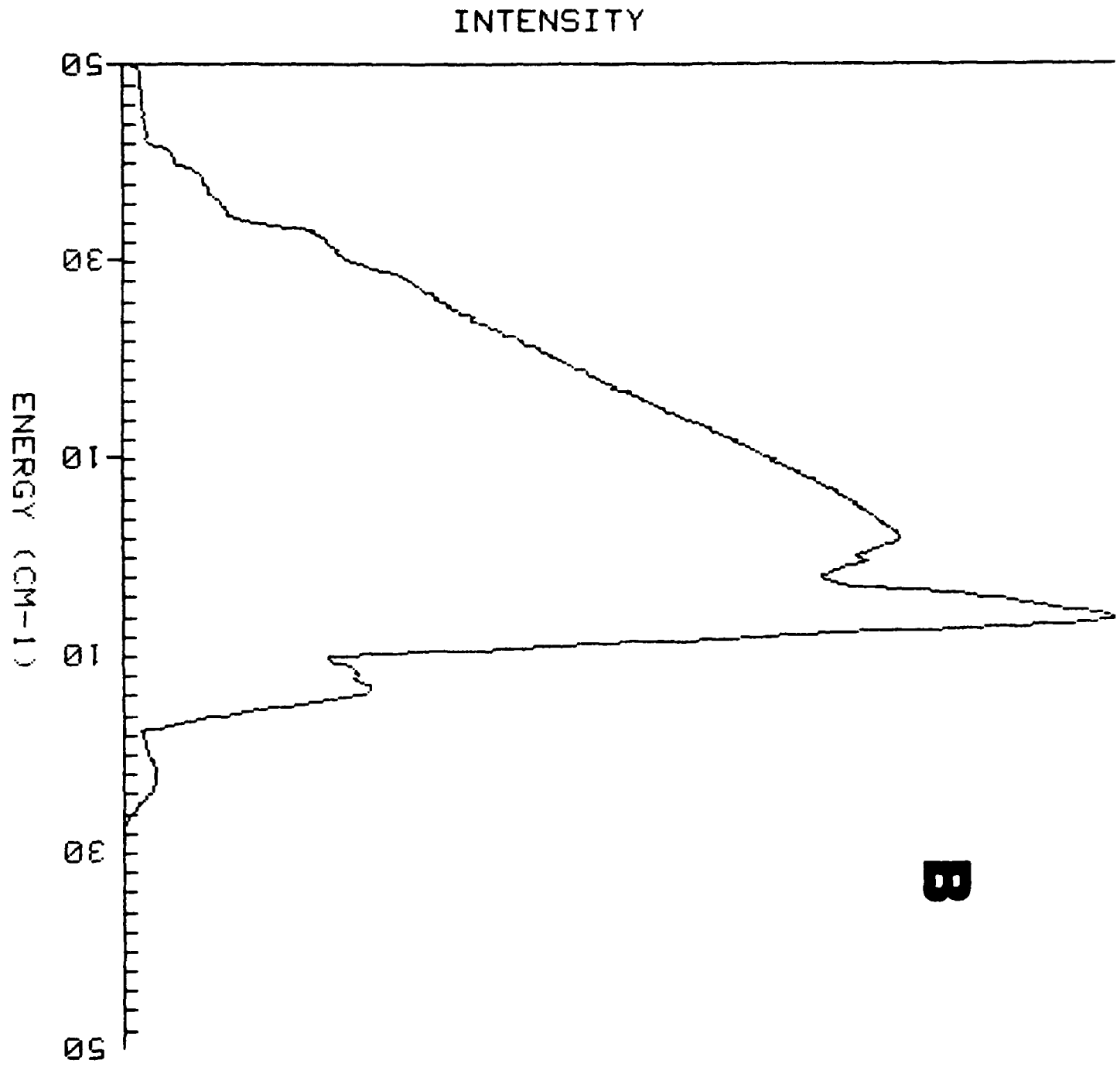

Fig 4B

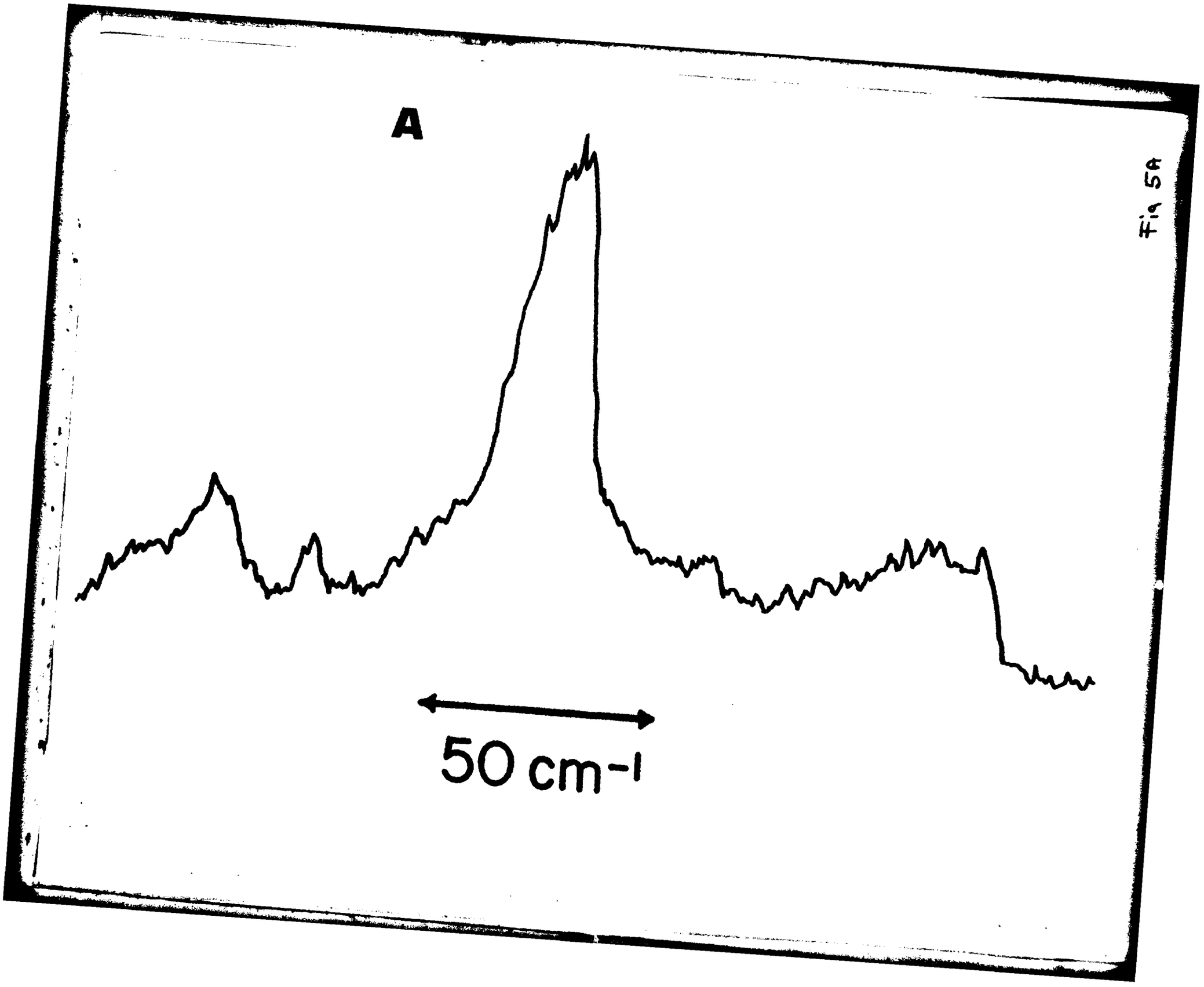
A
50 cm-1
Fig 5A

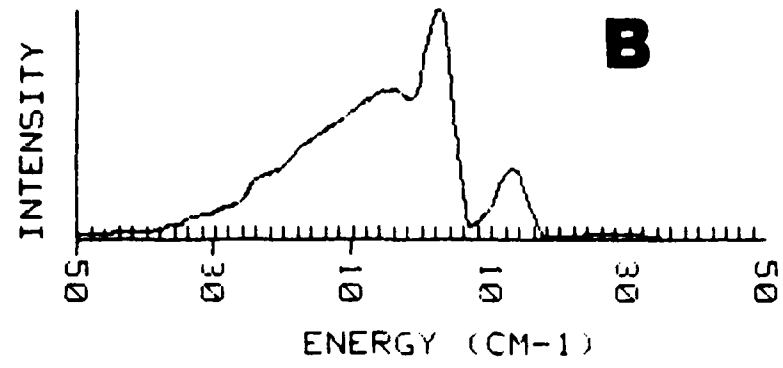
B
INTENSITY
ENERGY (CM-1)

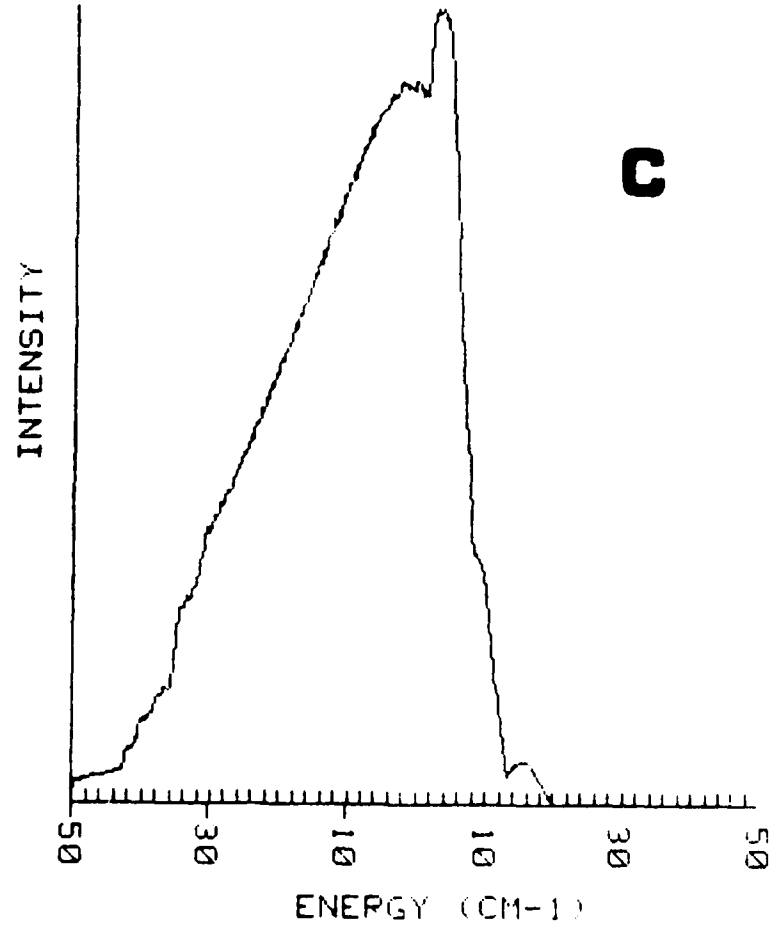
C
INTENSITY
ENERGY (CM-1)

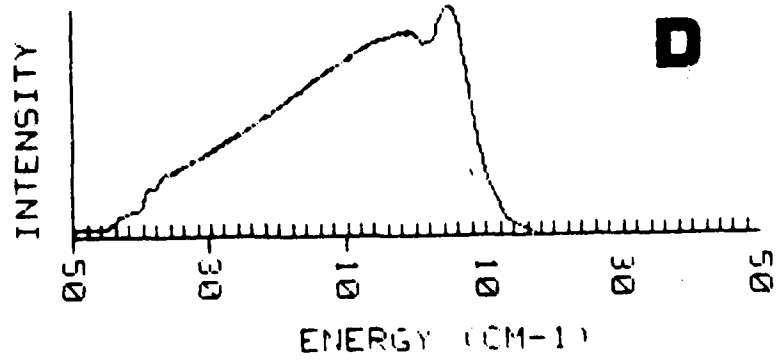
D
INTENSITY
ENERGY (CM-1)

Fig 5B,C,D

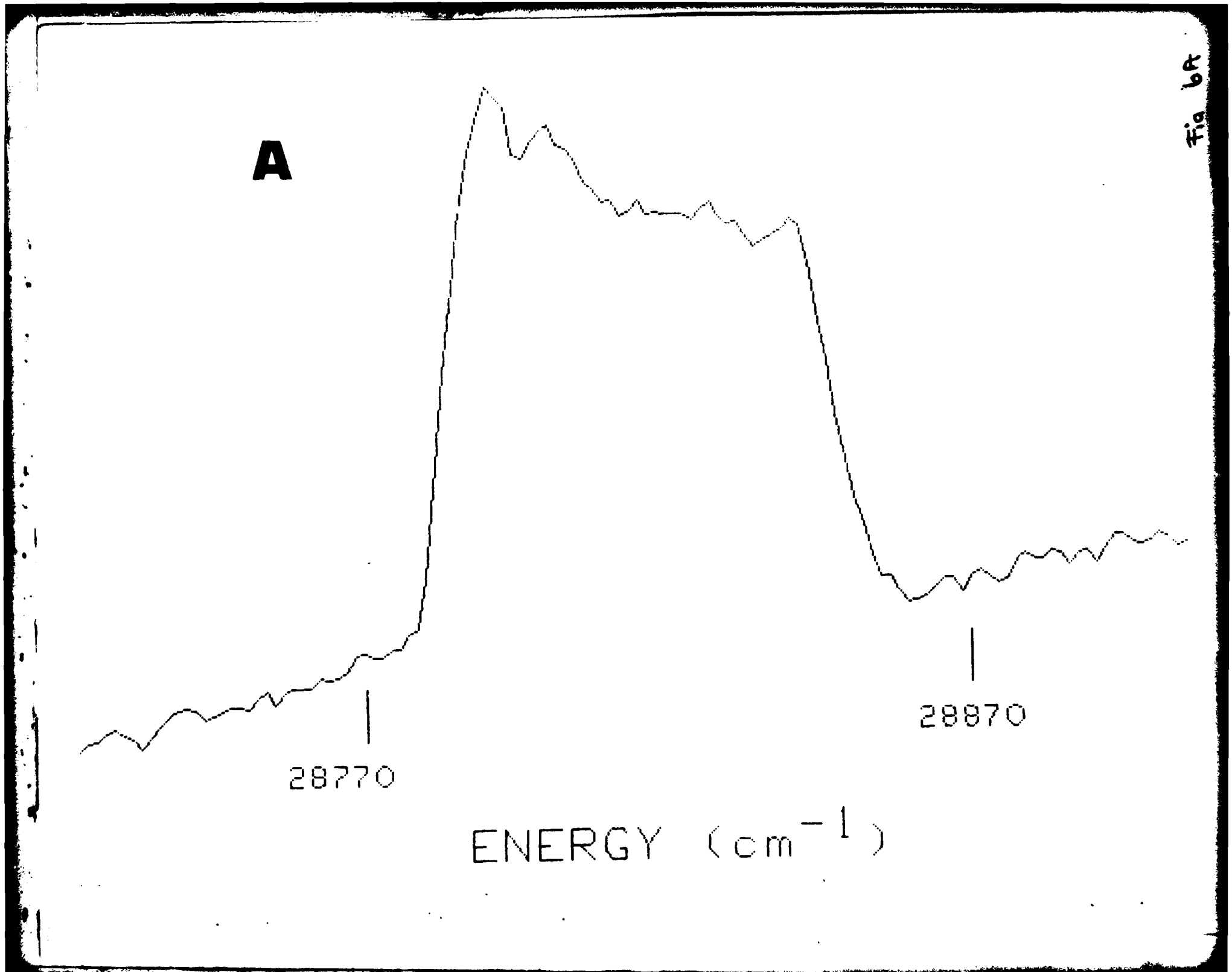
A
28770
28870
ENERGY (cm^{-1})
Fig 6A

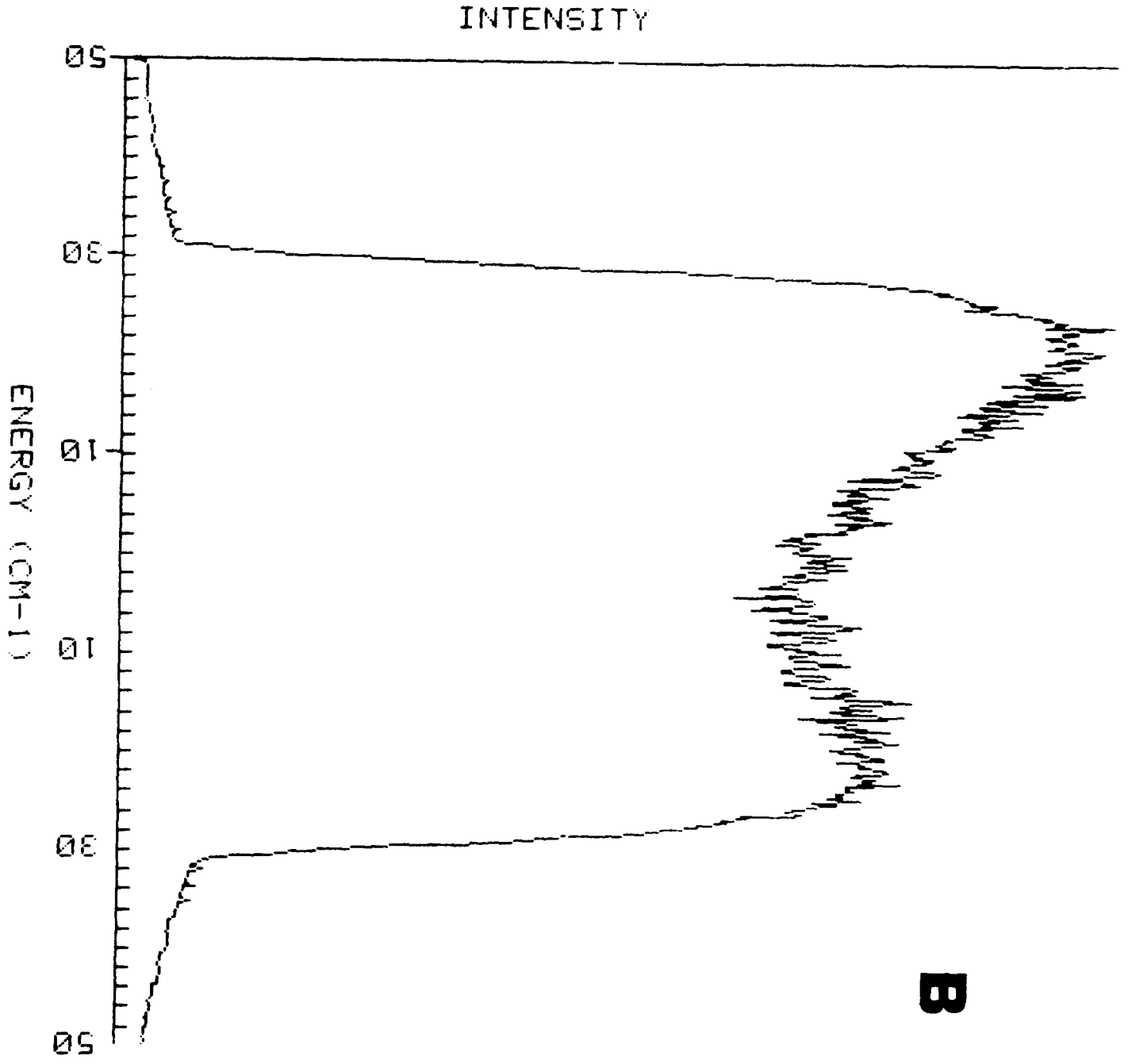

Fig 6B

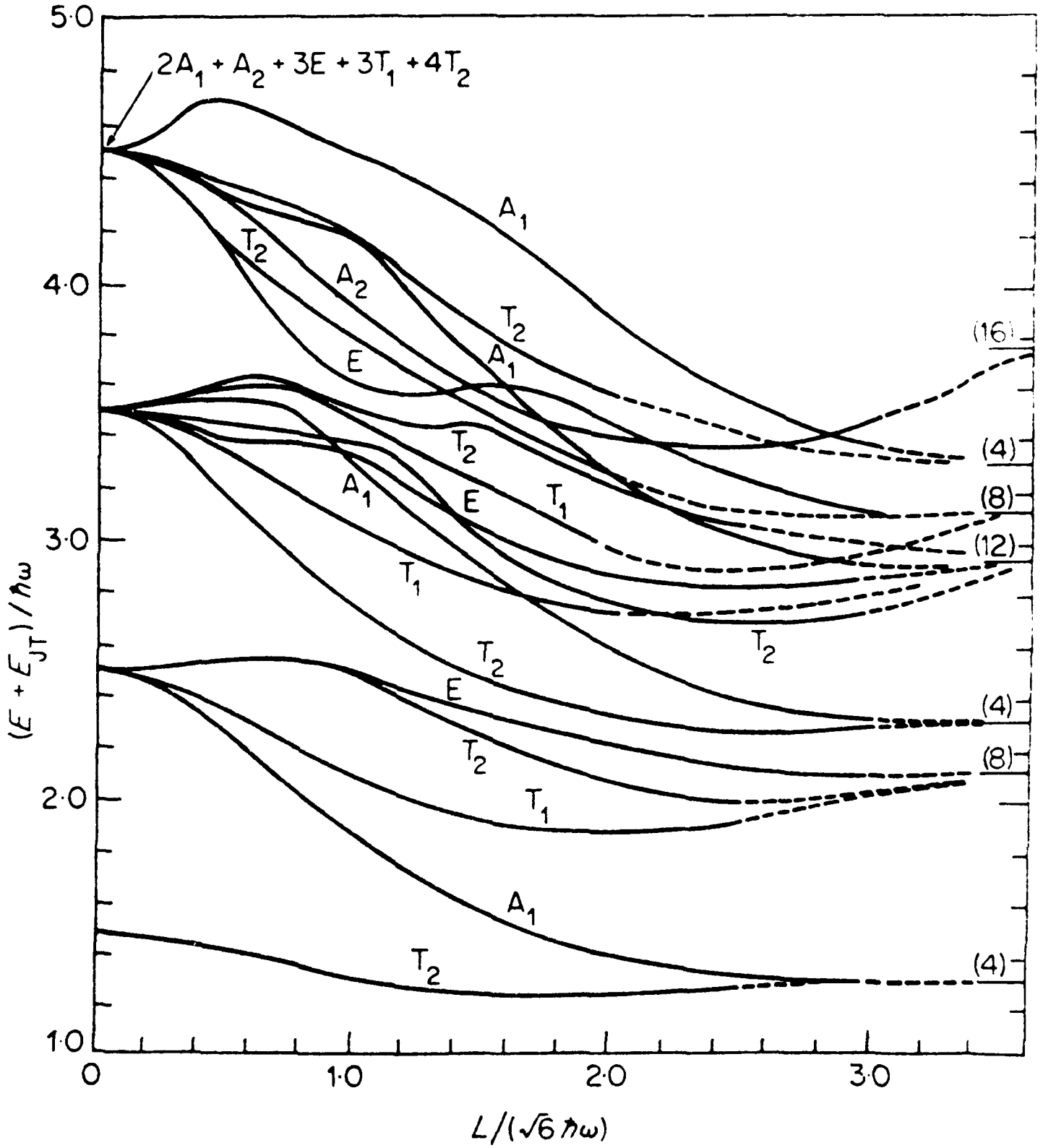
5·0
4·0
3·0
2·0
1·0
0
1·0
2·0
3·0
$(E + E_{JT})/\hbar\omega$
$L/(\sqrt{6}\hbar\omega)$
$2A_1 + A_2 + 3E + 3T_1 + 4T_2$
A_1
T_2
A_2
E
T_1
(16)
(4)
(8)
(12)

Fig 1